



# Bioconversion of waste glycerol for enhanced lipid accumulation in *Trichosporon shinodae*

S. P. Jeevan Kumar<sup>1,2,3</sup> · Vijay Kumar Garlapati<sup>4</sup> · Gujjala Lohit Kumar Srinivas<sup>5</sup> · Rintu Banerjee<sup>1</sup>

Received: 14 April 2021 / Revised: 30 June 2021 / Accepted: 19 July 2021

© The Author(s), under exclusive licence to Springer-Verlag GmbH Germany, part of Springer Nature 2021

## Abstract

Oleaginous yeast lipids have myriad of industrial applications that are gaining significant interest owing to shorter incubation, ability to use broad spectrum substrates, and quality lipids. However, the lipid content produced is low and need to enhance by optimization of varied parameters. In the present study, crude glycerol a by-product of biodiesel industry was supplemented to *Trichosporon shinodae* for lipid accumulation using central composite design (CCD) of response surface methodology (RSM). The developed quadratic model was found to be significant with the  $R^2$  value of 95.20% and adj.  $R^2$  value of 91.97%. An optimal lipid content of  $49.85 \pm 0.8\%$  (w/w) was obtained using *T. shinodae* with 6.2% (v/v) inoculum volume, pH 3.6, C/N ratio 105, 1.52 (g/L) of  $MgSO_4$ , and 4.55 mM  $FeSO_4$  in 120.72 h at 30 °C. Lipid composition from *T. shinodae* depicted the presence of linoleic acid (C18:2), oleic acid (C18:1), stearic acid (C18:0), palmitic acid (C18:0), myristic acid (C14:0), and lauric acids (C12:0), respectively. *T. shinodae* lipids have 61.1% (w/w) saturated fatty acids and unsaturated fatty acids proportion accord to 38.9% (w/w). Lipid composition of *T. shinodae* indicates that these lipids were suitable for synthesis of high value products like fuel additives, surfactants, detergents, and cleaning applications.



**Keywords** Fuel additive · Glycerol · Lipids · Oleaginous yeast · Surfactant · *T. shinodae*

## 1 Introduction

Yeast lipids also known as single cell oil (SCO) are the ideal substrates for surfactants, plasticizers, detergents, biofuels, and their additives production due to the high lipid productivity (> 20%), short cultivation period, and alleviates land requirement [1–3]. The yeast *T. shinodae* is capable to synthesize significant lipid content

under nitrogen-limited conditions with excess glycerol (a waste by-product from biodiesel unit) and agro-residues [4, 5]. However, succint supply of oleaginous lipids is a major drawback for commercial exploitation. To make the process viable, lipid accumulation using inexorbitant feedstocks and optimization of process parameters are quintessential.

Utilization of by-product crude glycerol is one of the best options for development of inexpensive process. Generally, crude glycerol is contaminated with methanol, water, oil, soap, and other compounds and has low autoignition quality, high viscosity, and poor lower heating value; as a result, it deems unsuitable neither for combustion use in fuel burners and internal combustion engines nor industrial chemicals (biorefinery) [6, 7]. In biodiesel production process, for every ton of biodiesel synthesis, 100 kg of raw glycerol (theoretical yield) is produced as a by-product in the transesterification process [8–10], which can be utilized for lipid accumulation using circular economy approach [7, 11, 12]. Oleaginous yeasts utilize glycerol to synthesize triglycerides through sequence conversion of glycerol to glycerol-3-phosphate (G-3-P), lipophosphatidic acid (LPA), phosphatidic acid

✉ Rintu Banerjee                 
rb@iitkgp.ac.in

<sup>1</sup> Agricultural and Food Engineering Department, Indian Institute of Technology, Kharagpur 721302, West Bengal, India

<sup>2</sup> ICAR-Indian Institute of Seed Science, Kushmaur, Mau 275103, U.P., India

<sup>3</sup> ICAR-Directorate of Floricultural Research, Pune 411036, Maharashtra, India

<sup>4</sup> Department of Biotechnology and Bioinformatics, Jaypee University of Information Technology, Waknaghat 173234, H.P., India

<sup>5</sup> Advanced Technology Development Centre, Indian Institute of Technology, Kharagpur 721302, India

(PA), diacyl glycerol and triglycerides using glycerol-3-phosphate acyltransferase, 1-acyl glycerol-3-phosphate acyltransferase, phosphatidic acid phosphatase, and diacylglycerol acyltransferase enzymes, respectively [13, 14].

To obtain higher lipid content, Wu et al. [15] have proposed a systematic approach of medium optimization from *T. capitatum* supplementing oleic acid as feedstock with the predominant variables of incubation time, pH, temperature, C/N ratio, and agitation speed. However, this conventional systematic approach of medium optimization for enhanced lipid content has failed to determine the interaction effects of different factors and usually end up with only one “apparent” set up of optimal conditions (local optima) [16].

To overcome this problem, mathematical-based RSM approach could be envisaged, where an empirical model has been developed through fitting of experimental data with the predicted data by taking interaction effects of controllable input variables on the observable output along with the anticipated optimized results [17, 18]. The efficiency of RSM in modeling and optimization of different biotechnological processes has been acknowledged in several research studies [19–21]. The pre-requisite condition for lipid accumulation in *T. shinodae* is the presence of higher carbon content coupled with nitrogen limitation [15, 22, 23]. In addition, some other factors such as inoculum volume, temperature, pH, trace elements concentration, and magnesium sulfate have showed their prominence in increasing lipid production. Hence, to increase the lipid content, the present study is aimed to optimize the process parameters that result in higher lipid production using crude glycerol a by-product in biodiesel industry [24, 25].

## 2 Materials and methods

### 2.1 Experimental material and chemicals

In this study, *T. shinodae* isolated, identified, and maintained in Microbial Biotechnology and Down Stream Processing laboratory, Agricultural and Food Engineering Department, Indian Institute of Technology, Kharagpur, India was used and maintained at regular intervals as enumerated by Kumar and Banerjee [4]. Fatty acids such as oleic, linoleic, lauric, palmitic, myristic, and stearic acids were procured from Sigma (USA). Besides, all the chemicals used in the study were procured from Qualigens, Merck and Himedia, India, which are of analytical grade.

### 2.2 Selection of variables by one-variable-at-a-time approach for optimization of lipid production in *T. shinodae*

Selection of influential parameters that determine the higher lipid content such as inoculum volume (1–20%, v/v), pH 1–12, carbon and nitrogen sources and their concentration (C/N ratio 1–200), magnesium sulfate (1–5 mg), ferrous sulfate (1–5 mM), and temperature (10–50 °C) were evaluated using OVAT approach. All experiments were done by altering the determinant concentration keeping other parameters range constant followed by biomass and lipid extraction.

### 2.3 Cell dry weight determination

After fermentation of every experiment, biomass harvesting was done by filtration and dried at 60 °C until constant weight is observed [4]. Dry cell weight was determined according to Kumar and Banerjee [19].

### 2.4 Extraction and quantification of lipid

The dried biomass was subjected to ultrasonication with a frequency of 50 Hz and 2800 W power for 20 min at 30 °C [19]. Lipid extraction was done from disrupted biomass using chloroform:methanol (2:1) according to Kumar and Banerjee [4]. Separation of the chloroform–methanol mixture into individual layers was performed as per Folch et al. [26], using 20 mL of sodium chloride (5%, w/v) and dispensed to a known weighed clean vial (W1). Thereafter, chloroform layer dispensed into vial (W1) was evaporated with a rotary evaporator (BUCHI Rotavapor R-124), and the vial weight with residue is recorded and designated as W2. Lipid content can be calculated by subtracting W1 from W2 and expressed as % dry cell weight [4].

### 2.5 Modelling and optimization for enhanced lipid content

To optimize the lipid production from the *T. shinodae*, influential experimental parameters such as incubation time (h), inoculum volume (v/v), pH, temperature (°C), MgSO<sub>4</sub> (mg/L), FeSO<sub>4</sub> (mg/L), and C/N ratio were studied as per the equation (Eq. 1) and are coded –1, 0, 1 as illustrated in Table 1. The experiments were designed using CCD of RSM by Minitab 16 (USA) statistical software to determine the effects of influential parameters on the lipid content (Table 2).

$$X = \frac{x - [X_{max} + X_{min}]/2}{[X_{max} - X_{min}]/2} \quad (1)$$

where  $x$  is the uncoded variable,  $X$  is the coded variable, and  $x_{\max}$  and  $x_{\min}$  are the maximum and minimum values of the uncoded variable. Employing RSM to fit the experimental data and to identify the relevant model terms, a second-order polynomial equation has been developed (Eq. 2) for a response (lipid content,  $Y_{\text{Lipid}}$ ) considering the individual, square, and interaction effects of seven production parameters as follows:

$$Y_{\text{lipid}} = b_0 + \sum_{i=1}^7 b_i A_i + \sum_{i=1}^7 \sum_{j=1}^7 b_{ij} A_i A_j + \sum_{i=1}^7 b_{ij} A_i^2 + \epsilon \tag{2}$$

where  $b_0$  being intercept,  $b_i$  corresponds to first order,  $b_{ij}$  represents interactive, and  $b_{ii}$  is second-order effects, while  $\epsilon$  directs towards residual error,  $i$  and  $j$  represent the factor number of factors [16, 27].

The experimental conditions adopted for development of RSM was tabulated in Table 2.

### 2.6 Validation of the model

The accuracy and validation of the model were evaluated by ANOVA test using Fisher’s test ( $F$ -test) heuristics. The significance of individual, square and interaction effects of lipid production parameters on the lipid content ( $Y_{\text{Lipid}}$ ) was identified by statistically significant  $P$  values  $< 0.05$  with 95% confidence interval. The predicted output with the set of production parameters was further utilized to test through triplicate experimental runs [28]. The accuracy of the model further assessed through the coefficient of determination ( $R^2$ ) and adjusted  $R^2$  values. The applicability of the developed model also evaluated for lack of fit.

### 2.7 Interaction study of parameters and their optimization

The interaction effects of influential parameters on lipid yield presented through the 3D surface plots. Finally, the attainment of maximum lipid yield through possible values

of important parameters predicted through the optimizer function of RSM.

## 2.8 Derivatization and characterization of microbial lipids

### 2.8.1 GC–MS based lipid characterization of *T. shinodae*

Lipids estimation was carried out using GC–MS instrument with gas chromatography unit (Agilent 6890 N) and mass detector (Agilent MS-5975 inert XL). The capillary column employed was HP-5-MS with dimensions of 30 m × 0.25 mm × 0.25 mm film thickness. A program for the lipids estimation was set according to Kumar and Banerjee [4], and the lipid analysis was done using National Institute of Standards and Technology (NIST) library.

### 2.8.2 FT-IR characterization of lipids derived from *T. shinodae*

Lipids derived from *T. shinodae* were characterized using FT-IR as per Forfang et al. [29] protocol. In this study, Bruker quinox FT-IR spectrometer with mercury-cadmium-telluride detector was used. Sample preparation and analysis was done in triplicate according to Forfang et al. [29], and the spectra of lipids were retrieved in the wave number range of 4000–600  $\text{cm}^{-1}$ .

### 2.8.3 Determination of lipid properties derived from *T. shinodae*

Fatty acids quality is an important factor which depends on the feedstock. Fatty acids chain length, unsaturation, and free fatty acids content are important determinants of combustion properties and oxidative stability [30]. Acid value (AV), saponification value (SV), and iodine value (IV) of *T. shinodae* are important parameters to determine the quality of lipids. These are determined as per the procedure enumerated in Kumar and Banerjee [4].

**Table 1** Experimental range of variables for the CCD of RSM in actual and coded variables for lipid (single-cell oil) production

Variables	Symbol coded	Range of variables		
		Low (−1)	Mid (0)	High (+1)
Incubation time (IT, h)	A	96	120	144
Inoculum volume (IV, % v/v)	B	3	5	7
pH	C	3	3.5	4
Temperature (temp, °C)	D	25	30	35
MgSO <sub>4</sub> (g/L)	E	1	1.5	2
FeSO <sub>4</sub> (mM)	F	3	4	5
C/N ratio	G	100	120	140

**Table 2** Experimental runs of CCD of RSM along with the experimental and predicted values of lipid yield (%)

Experimental run	IT <sup>a</sup> (h)	IV <sup>b</sup> (%)	pH	Temp <sup>c</sup> (°C)	MgSO <sub>4</sub> (g/L)	FeSO <sub>4</sub> (mM)	C/N ratio	Lipid yield (%)	
								Exp.	<sup>d</sup> predict. <sup>e</sup>
1	96	3	4	35	1	3	140	44.11	44.05
2	120	5	3.5	25	1.5	4	120	43.88	42.52
3	120	5	3.5	30	1.5	4	140	47.78	47.87
4	120	5	3.5	30	1.5	4	120	46.05	46.21
5	120	5	3.5	35	1.5	4	120	41.92	42.93
6	96	3	4	25	2	5	100	46.67	46.37
7	144	3	3	35	2	5	140	42.93	43.36
8	144	7	3	35	2	5	100	47.00	46.70
9	144	7	4	25	2	3	140	41.98	42.32
10	96	7	4	35	2	3	140	43.33	43.93
11	144	3	3	25	1	5	140	44.12	43.91
12	144	3	3	25	1	3	100	46.08	45.65
13	96	3	3	25	2	5	140	41.50	41.86
14	96	5	3.5	30	1.5	4	120	46.06	45.49
15	144	7	4	25	1	3	100	47.11	46.40
16	96	3	4	35	2	5	140	43.15	42.98
17	96	7	3	25	1	3	100	43.74	44.02
18	144	3	4	35	1	3	100	45.10	45.28
19	96	7	3	35	2	5	140	46.45	46.07
20	96	7	3	35	1	3	140	42.20	41.87
21	144	7	4	25	1	5	140	46.99	47.72
22	96	7	4	25	2	5	140	42.90	43.18
23	144	3	4	25	1	5	100	48.34	48.36
24	120	5	3.5	30	1.5	3	120	48.51	48.11
25	120	5	3.5	30	1	4	120	43.93	44.28
26	96	3	3	25	2	3	100	48.01	47.76
27	144	7	3	25	2	3	100	44.98	45.41
28	96	7	4	25	2	3	100	45.91	46.03
29	144	3	3	25	2	3	140	41.91	41.36
30	144	3	3	35	1	5	100	43.44	42.68
31	96	7	4	25	1	5	100	48.33	48.10
32	144	7	3	35	1	3	100	42.93	43.39
33	144	7	4	35	2	3	100	47.07	46.67
34	144	3	4	35	1	5	140	47.08	46.85
35	120	5	3.5	30	1.5	5	120	48.82	48.87
36	144	7	4	35	2	5	140	48.38	48.33
37	144	7	4	25	2	5	100	47.14	46.77
38	144	3	4	25	1	3	140	44.91	45.11
39	144	3	4	25	2	5	140	42.13	41.69
40	144	3	4	35	2	5	100	43.37	43.31
41	120	5	3.5	30	1.5	4	100	50.16	49.72
42	96	7	3	35	1	5	100	44.04	43.63
43	96	7	3	35	2	3	100	47.90	47.41
44	120	5	3.5	30	2	4	120	44.53	43.83
45	96	3	3	35	1	3	100	44.83	44.98
46	96	3	3	35	1	5	140	44.03	43.56
47	96	7	4	25	1	3	140	42.15	41.91
48	96	3	3	35	2	5	100	44.26	45.06

**Table 2** (continued)

Experimen- tal run	IT <sup>a</sup> (h)	IV <sup>b</sup> (%)	pH	Temp <sup>c</sup> (°C)	MgSO <sub>4</sub> (g/L)	FeSO <sub>4</sub> (mM)	C/N ratio	Lipid yield (%)	
								Exp.	<sup>d</sup> predict. <sup>e</sup>
49	96	3	4	25	1	5	140	45.73	46.28
50	144	3	3	25	2	5	100	43.00	43.38
51	144	7	4	35	1	5	100	47.29	47.43
52	96	3	4	35	1	5	100	46.04	46.26
53	96	3	4	25	1	3	100	49.22	49.22
54	144	7	3	35	2	3	140	46.63	46.67
55	144	7	3	25	2	5	140	44.22	43.75
56	120	5	3.5	30	1.5	4	120	46.15	46.21
57	120	5	3.5	30	1.5	4	120	46.15	46.21
58	144	3	3	35	1	3	140	43.51	43.85
59	96	7	3	25	2	5	100	46.4	46.44
60	120	5	3.5	30	1.5	4	120	46.05	46.21
61	144	5	3.5	30	1.5	4	120	45.40	45.61
62	96	7	4	35	1	5	140	46.56	46.24
63	144	7	3	25	1	3	140	42.19	41.91
64	96	3	4	35	2	3	100	46.15	45.58
65	96	7	4	35	1	3	100	44.02	44.61
66	144	3	3	35	2	3	100	45.16	44.76
67	120	7	3.5	30	1.5	4	120	48.15	48.36
68	120	5	3	30	1.5	4	120	43.48	43.91
69	96	7	3	25	2	3	140	41.13	41.48
70	120	5	4	30	1.5	4	120	45.76	44.98
71	120	5	3.5	30	1.5	4	120	46.05	46.21
72	96	3	4	25	2	3	140	41.34	40.97
73	96	3	3	25	1	5	100	47.01	47.0
74	96	7	3	25	1	5	140	42.57	42.34
75	96	3	3	35	2	3	140	44.0	44.08
76	96	7	4	35	2	5	100	46.87	47.33
77	120	5	3.5	30	1.5	4	120	46.12	46.21
78	120	5	3.5	30	1.5	4	120	46.05	46.21
79	144	7	3	25	1	5	100	44.27	44.72
80	120	5	3.5	30	1.5	4	120	45.95	46.21
81	144	3	4	35	2	3	140	42.66	42.85
82	144	7	3	35	1	5	140	45.75	46.22
83	120	5	3.5	30	1.5	4	120	45.11	46.21
84	144	7	4	35	1	3	140	46.91	46.17
85	144	3	4	25	2	3	100	43.21	44.60
86	120	5	3.5	30	1.5	4	120	46.25	46.21
87	120	3	3.5	30	1.5	4	120	48.32	47.76
88	96	3	3	25	1	3	140	42.71	43.23

IT<sup>a</sup>, Incubation time (h); IV<sup>b</sup>, inoculum value (% v/v); Temp<sup>c</sup>, temperature (°C); Exp<sup>d</sup>, experimental; <sup>e</sup>Predicted, predicted

## 2.8.4 Statistical analysis

All the experiments were done in triplicates and the standard error was calculated at 5% level.

## 3 Results and discussion

### 3.1 Development and analysis of the RSM model for lipid production

In this study, lipid production from *T. shinodae* was executed based on the CCD sets of RSM and evaluated with MINITAB 16.0 (USA) software. A quadratic non-linear polynomial equation was developed based on the positive and negative effects in the regression coefficients of the individual, square, and interaction terms of the production parameters. The production parameters, whose *P* values are < 0.05, were considered as the significant for the non-linear regression equation (Eq. 3). The predicted response of lipid yield was calculated by Eq. (3) as given below:

$$\begin{aligned}
 \text{Lipid yield}(\%) = & 4.2 + 0.042IT(h) - 9.41IV(\%, v/v) \\
 & + 51.8pH + 7.151Temp(^{\circ}C) + 32.68MgSO_4(g/L) \\
 & - 21.81FeSO_4(mM) - 1.942C/Nratio - 0.001141IT(h) \\
 & \times IT(h) + 0.4628IV(\%, v/v) \times IV(\%, v/v) \\
 & - 7.05pH \times pH - 0.1394Temp(^{\circ}C) \times Temp(^{\circ}C) \\
 & - 8.62MgSO_4(g/L) \times MgSO_4(g/L) + 2.282FeSO_4(mM) \\
 & \times FeSO_4(mM) + 0.006456C/Nratio \\
 & \times C/Nratio + 0.00918IT(h) \times IV(\%, v/v) \\
 & + 0.01283IT(h) \times pH + 0.001305IT(h) \times Temp(^{\circ}C) \\
 & - 0.01691IT(h) \times MgSO_4(g/L) + 0.00080IT(h) \\
 & \times FeSO_4(mM) + 0.001053IT(h) \times C/Nratio \\
 & + 0.1225IV(\%, v/v) \times pH + 0.04283IV(\%, v/v) \\
 & \times Temp(^{\circ}C) + 0.5953IV(\%, v/v) \times MgSO_4(g/L) \\
 & + 0.1968IV(\%, v/v) \times FeSO_4(mM) + 0.00365IV(\%, v/v) \\
 & \times C/Nratio - 0.0452pH \times Temp(^{\circ}C) - 2.480pH \\
 & \times MgSO_4(g/L) + 0.583pH \times FeSO_4(mM) - 0.00669pH \\
 & \times C/Nratio + 0.1908Temp(^{\circ}C) \times MgSO_4(g/L) + 0.0144Temp(^{\circ}C) \\
 & \times FeSO_4(mM) + 0.006757Temp(^{\circ}C) \times C/Nratio \\
 & - 0.467MgSO_4(g/L) \times FeSO_4(mM) - 0.02842MgSO_4(g/L) \\
 & \times C/Nratio + 0.01624FeSO_4(mM) \times C/Nratio
 \end{aligned} \tag{3}$$

In the predicted response of lipid yield equation, the +ve signs indicate the synergistic effects, while -ve signs denote the antagonistic effects of the production parameters on the response, i.e., lipid yield (% w/w).

### 3.2 Statistical validation of the model

The ANOVA results for a quadratic model of lipid yield showed the significant effect of individual, square, and interaction terms of production variables on the lipid yield (Table 3). Based on the presumption of terms, interactions between parameters with *P* < 0.05 were considered as significant terms, whereas *P* > 0.05 were deemed to be insignificant [31]. Among all terms, only individual and square terms of incubation time, interaction terms of incubation time and FeSO<sub>4</sub>, inoculum volume and pH, inoculum volume and C/N ratio, pH and temperature, and pH and C/N ratio were found to be insignificant (*P* > 0.05) on the lipid yield. The remaining all individual, square, and interaction terms of the quadratic model were found to be significant (*P*-value < 0.05) on the lipid yield from *T. shinodae*. The significant effects of pH, temperature, C/N ratio, FeSO<sub>4</sub>, and MgSO<sub>4</sub> resulted higher lipid accumulation in *T. shinodae* [32].

The significance of quadratic model terms on lipid yield was drawn from the *F*-values of the ANOVA results, where the large *F*-values of the quadratic model were considered as a highly significant model [33]. Based on the magnitude of the *F*-values, the production parameters namely pH, temperature, C/N ratio, FeSO<sub>4</sub>, and MgSO<sub>4</sub> were found to be influential parameters on the lipid production for *T. shinodae* using glycerol as carbon source. The significance of the statistical model depends on the *R*<sup>2</sup> and adj. *R*<sup>2</sup> values of the model. The *R*<sup>2</sup> value of more than 75% suggests that the optimization model is highly significant [34]. In this study, the *R*<sup>2</sup> value for lipid accumulation in *T. shinodae* using glycerol is 95.20%, which signifies that the model is highly significant.

The significance and adequacy of the statistical model could be drawn from the ranges of *R*<sup>2</sup> and adj. *R*<sup>2</sup> values [35]. For a good agreement, the *R*<sup>2</sup> and adj. *R*<sup>2</sup> values need to be within 20% range. The *R*<sup>2</sup> value of the developed quadratic model for lipid yield (95.20%) was close to the 100%, which implies that the model offers 95.2% variability in predicting lipid yield (%) apart from the experimental interval of production parameters. The *R*<sup>2</sup> (95.20%) value of the model was very close to the adjusted *R*<sup>2</sup> value (91.97%), which indicates the fitness of the developed model and negligible proportion of the variation between the experimental and predicted data. The fitness and significance of the developed regression model through *R*<sup>2</sup> and adj. *R*<sup>2</sup> values have been reported in the studies [19, 35]. From these results, it has concluded that the developed RSM model satisfactorily predicted the lipid yield from the taken set of production parameters.

**Table 3** ANOVA analysis for quadratic model of lipid yield (%) from *Trichosporon shinodae*

Source	DF	Adj SS	AdjMS	F-value	P-value	Status
Model	35	366.424	10.4693	29.48	0.000	Significant
Linear	7	97.175	13.8822	39.10	0.000	Significant
IT (h)	1	0.226	0.2259	0.64	0.429	Not significant
IV (% v/v)	1	5.786	5.7862	16.30	0.000	Significant
pH	1	19.043	19.0431	53.63	0.000	Significant
Temp (°C)	1	2.681	2.6806	7.55	0.008	Significant
MgSO <sub>4</sub> (g/L)	1	3.396	3.3964	9.57	0.003	Significant
FeSO <sub>4</sub> (mM)	1	9.578	9.5776	26.97	0.000	Significant
C/N ratio	1	56.466	56.4657	159.02	0.000	Significant
Square	7	97.405	13.9150	39.19	0.000	Significant
IT (h)×IT (h)	1	1.005	1.0053	2.83	0.098	Not significant
IV (% v/v)×IV (% v/v)	1	7.969	7.9693	22.44	0.000	Significant
pH×pH	1	7.229	7.2286	20.36	0.000	Significant
Temp (°C)×Temp (°C)	1	28.239	28.2388	79.53	0.000	Significant
MgSO <sub>4</sub> (g/L)×MgSO <sub>4</sub> (g/L)	1	10.791	10.7906	30.39	0.000	Significant
FeSO <sub>4</sub> (mM)×FeSO <sub>4</sub> (mM)	1	12.113	12.1125	34.11	0.000	Significant
C/N ratio×C/N ratio	1	15.513	15.5125	43.69	0.000	Significant
2-Way Interaction	21	171.844	8.1830	23.05	0.000	Significant
IT (h)×IV (% v/v)	1	12.420	12.4203	34.98	0.000	Significant
IT (h)×pH	1	1.518	1.5178	4.27	0.044	Significant
IT (h)×Temp (°C)	1	1.570	1.5700	4.42	0.040	Significant
IT (h)×MgSO <sub>4</sub> (g/L)	1	2.635	2.6349	7.42	0.009	Significant
IT (h)×FeSO <sub>4</sub> (mM)	1	0.024	0.0239	0.07	0.796	Not significant
IT (h)×C/N ratio	1	16.340	16.3398	46.02	0.000	Significant
IV (% v/v)×pH	1	0.961	0.9609	2.71	0.106	Not significant
IV (% v/v)×Temp (°C)	1	11.743	11.7426	33.07	0.000	Significant
IV (% v/v)×MgSO <sub>4</sub> (g/L)	1	22.681	22.6814	63.88	0.000	Significant
IV (% v/v)×FeSO <sub>4</sub> (mM)	1	9.911	9.9115	27.91	0.000	Significant
IV (% v/v)×C/N ratio	1	1.363	1.3631	3.84	0.055	Not significant
pH×Temp (°C)	1	0.816	0.8163	2.30	0.136	Not significant
pH×MgSO <sub>4</sub> (g/L)	1	24.604	24.6041	69.29	0.000	Significant
pH×FeSO <sub>4</sub> (mM)	1	5.445	5.4452	15.34	0.000	Significant
pH×C/N ratio	1	0.286	0.2865	0.81	0.373	Not significant
Temp (°C)×MgSO <sub>4</sub> (g/L)	1	14.560	14.5599	41.01	0.000	Significant
Temp (°C)×FeSO <sub>4</sub> (mM)	1	0.332	0.3324	0.94	0.338	Not significant
Temp (°C)×C/N ratio	1	29.222	29.2221	82.30	0.000	Significant
MgSO <sub>4</sub> (g/L)×FeSO <sub>4</sub> (mM)	1	3.488	3.4885	9.82	0.003	Significant
MgSO <sub>4</sub> (g/L)×C/N ratio	1	5.169	5.1688	14.56	0.000	Significant
FeSO <sub>4</sub> (mM)×C/N ratio	1	6.754	6.7535	19.02	0.000	Significant
Error	52	18.464	0.3551			
Lack-of-fit	43	17.524	0.4075	3.90	0.017	Significant
Pure error	9	0.939	0.1044			
Total	87	384.888				

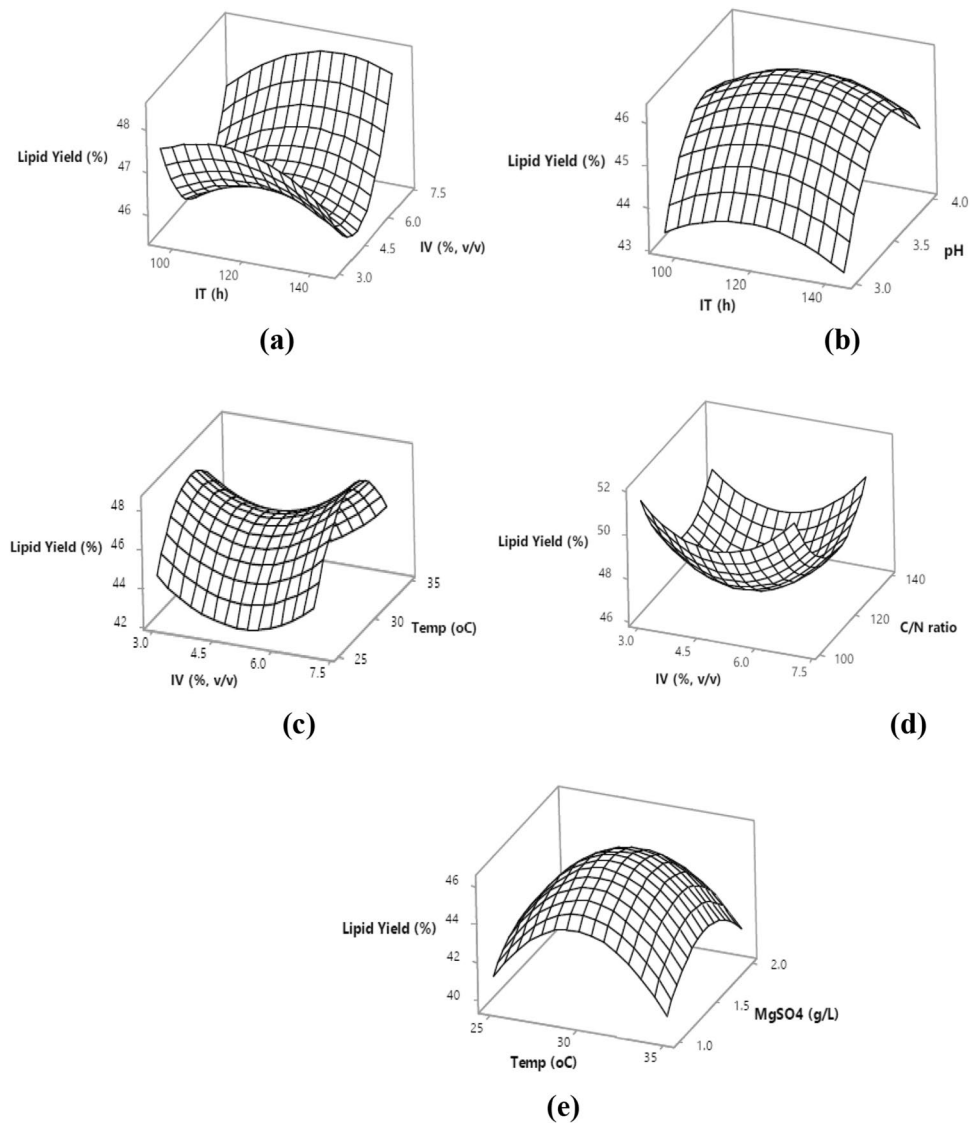
S=0.595882 R-Sq=95.20% R-Sq(adj)=91.97%

### 3.3 Response surface plots analysis

The 3D response surface plots of RSM (drawn through MINITAB 16) help in investigating the interaction effects of different production variables on the lipid yield (Fig. 1).

The interaction effect of the incubation time (IT) and inoculum volume (IV) on lipid yield (%) is illustrated in Fig. 1(a). The higher lipid yield seems with the mid-range of incubation time (around 120 h) and more upper side of inoculum volume. This type of behavior is attributed to the

**Fig. 1** Response surface plots of lipid yield (%) with **a** incubation time (IT, h) and inoculum volume (IV, % v/v); **b**) incubation time ((IT, h) and pH; **c**) inoculum volume (IV, % v/v) and temperature ( $^{\circ}\text{C}$ ); **d**) inoculum volume (IV, % v/v) and C/N ratio (%); **e** temperature ( $^{\circ}\text{C}$ ) and  $\text{MgSO}_4$  (g/L)



exhausting of the substrate with the incubation time and higher inoculum volumes needed for initiating the *T. shinodae* growth for the higher lipid production.

Interaction effect of incubation time (IT) and pH on the lipid yield depicted in Fig. 1(b) implies that the substantial lipid yield observed with the mid-range of incubation time (120 h) and pH value of around 3.6. The interaction results suggested that the higher lipid yield was possible with the mid-range of incubation time that is required to reach the exponential phase of the lipid production with the production medium pH around 3.6.

From the interaction effect of inoculum volume (IV) and temperature of lipid yield (Fig. 1(c)), it was found that higher range side of inoculum volume coupled with temperature at  $30^{\circ}\text{C}$  was the ideal for maximum SCO production. Similar results was observed with *T. capitatum*,

where the maximum lipid accumulation has been increased up to  $28^{\circ}\text{C}$  and further increase in temperature lead to sharp decline of lipid accumulation [15]. This observed pattern is due to the partial inactivation of lipid synthesis enzymes at higher temperature. The fate of lipid yield based on the interaction effects of inoculum volume and C/N ratio is summarized in Fig. 1(d). The response plot indicates that the maximum ranges of inoculum volume and C/N ratio significantly contributed for higher lipid yields owing to higher C/N ratio and inoculum volume that facilitate the growth of the *T. shinodae*.

Finally, Fig. 1(e) depicts the interaction effect of temperature and  $\text{MgSO}_4$  on lipid yield. From the response surface plot, the mid-range values of temperature and  $1.52$  (g/L) of  $\text{MgSO}_4$  were the ideal for higher lipid yields. Divalent metal ions play a significant role in increasing the lipid production



by binding and stabilizing the malic enzyme, which is a rate limiting step in fatty acid biosynthesis [36]. Further increase of  $\text{MgSO}_4$  resulted decrease of SCO accumulation in *T. shinodae* due to divalent toxicity and higher range of temperature.

### 3.4 Optimization towards higher lipid yields and experimental validation

The response optimizer function (MINITAB 16) predicated a lipid yield of 50.12% with the incubation time of 120.72 h, 6.2 (% v/v) inoculum volume, C/N ratio of 105 at 30 °C using pH 3.6, 1.52 (g/L) of  $\text{MgSO}_4$  and 4.55 mM of  $\text{FeSO}_4$ . The predicted set of production variables were done in triplicate for experimental validation. The experimental lipid yield was found to be  $49.85 \pm 0.8\%$  that was found to be in good agreement with the predicted optimum. The optimal lipid yields from *T. shinodae* using various parameters (variables) is in good agreement with other optimization studies that have employed glycerol as a carbon source [15, 19, 36]. Saenge et al. [13] reported 42.12% (w/w) of lipid content from *Rhodotorula glutinis* using glycerol with optimized parameters of C/N ratio 85, pH 6, and aeration rate 2vvm. Similarly, Saenge et al. [37] obtained 48.90% (w/w) of lipid content with two-stage lipid production from *Rhodospiridium toruloides* Y4 in glycerol (50 g/L) supplemented broth coupled with optimized cultural parameters of pH 6 and inoculum volume 20 mL. These studies substantiate that the production parameters have a potential for enhanced lipid accumulation and are in corroboration with the present study findings. Similar findings were observed in studies pertinent to lipid production using optimization of process parameters [13, 21].

### 3.5 Lipid profiling of *T. shinodae* using GC–MS

The lipids obtained by optimization of different variables were determined their quality using GC–MS analysis. *T. shinodae* fatty acids using GC–MS depicted the presence

of linoleic acid (C18:2), oleic acid (C18:1), stearic acid (C18:0), palmitic acid (C16:0), myristic acid (C14:0), and lauric acids (C12:0), respectively (Table 4). The proportion of saturated fatty acids was 61.1% and unsaturated fatty acids content remained 38.9%, respectively. Among polyunsaturated fatty acids, presence of oleic acid is highly preferable because of low melting point ( $-19.9$  °C) that enhance fuel additive properties at low temperatures and storage [38]. Lipid composition of oleaginous yeast determines the quality of oleochemicals. Fatty acids properties such as chain length, saturation, and unsaturation and branching influence the properties. Fatty acid with long chain length has good ignition property that can be used as fuel additive. However, longer chain length with more unsaturation decreases ignition property and prone to oxidation [39, 40]. On the other hand, polyunsaturated fatty acids (PUFA) reduce cetane number, stability, cloud point, and increase in NOx emission. *T. shinodae* lipids being rich in oleic acid can be used as fuel additive.

### 3.6 FT-IR characterization of lipids obtained from *T. shinodae*

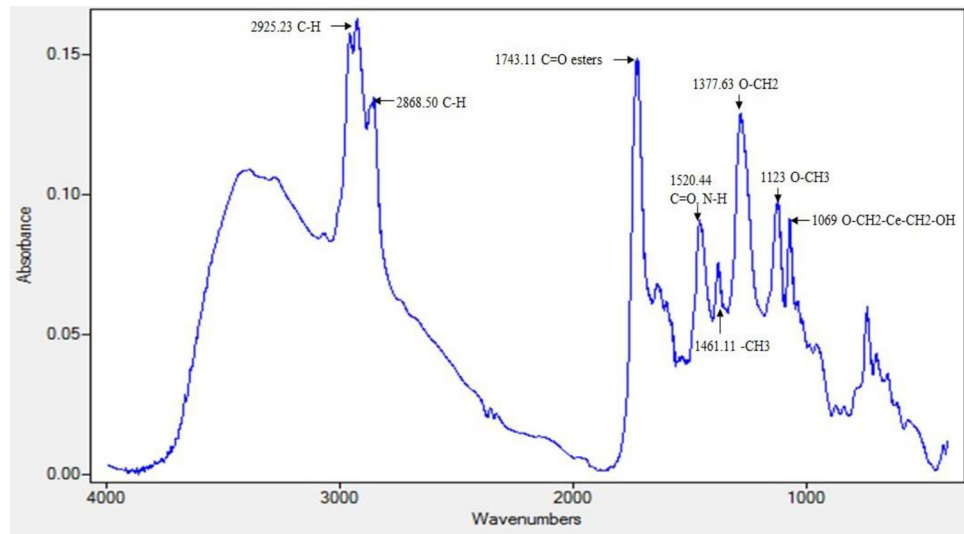
The lipids of *T. shinodae* can be identified with the peaks at  $2952.23\text{ cm}^{-1}$  and  $2868.50\text{ cm}^{-1}$  because of symmetric and asymmetric aliphatic C–H stretching [41]. A peak at  $1743.11\text{ cm}^{-1}$  signifies C=O ester groups by virtue of lipids and fatty acids and peaks at  $1520.44\text{ cm}^{-1}$  corresponds to N–H amides of proteins that was probably derived from residual biomass proteins obtained in the extraction process [42]. The fingerprint region of the compounds provides specific pattern in the region of  $1500\text{--}900\text{ cm}^{-1}$ . The peak at  $1461.11\text{ cm}^{-1}$  corresponds to asymmetric stretching of  $-\text{CH}_3$  group of long chain fatty acids [43]. Similarly, peaks at  $1377.63\text{ cm}^{-1}$ ,  $1123\text{ cm}^{-1}$ , and  $1069\text{ cm}^{-1}$  imply the presence of  $\text{O}-\text{CH}_2-$ ,  $\text{O}-\text{CH}_3$  groups that correspond to tri, di, and monoglycerides, respectively [44] (Fig. 2).

**Table 4** *T. shinodae* lipid composition and their evaluation with other predominant oil composition

Oil/lipid source	C:8	C:10	C:12	C:14	C:16	C:18:0	C:18:1	C:18:2	C:18:3	C:20	C:22
Canola	-	-	-	-	3.9	1.9	64.1	18.7	9.2	0.6	0.2
Cocoa Butter	-	-	-	0.1	25.8	34.5	35.3	2.9	-	1.1	-
Coconut	8.0	6.4	48.5	17.6	8.4	2.57	6.5	1.5	-	0.1	-
Linseed	-	-	-	-	4.8	4.7	19.9	15.9	52.7	-	1.1
Olive	-	-	-	-	13.7	2.5	71.1	10.0	0.6	0.9	-
Palm	-	-	0.3	1.1	45.1	0.1	4.7	38.8	9.4	0.3	-
Peanut	-	-	-	0.1	11.6	3.1	46.5	31.4	-	1.5	3
Soybean	-	-	-	0.1	11.0	4.0	23.4	53.2	7.8	0.3	0.1
<i>T. shinodae</i>	-	-	6.1	10.0	40.0	5.0	35.0	3.9	-	-	-

Oil composition of vegetable oils has been retrieved from Tao [51]

**Fig. 2** FT-IR spectra of *T. shinodae* lipids



## 4 Biochemical properties of *T. shinodae* lipids

### 4.1 Acid value

Biochemical properties of *T. shinodae* have been done with acid value, iodine value, and saponification value (Table 5). Acid value signifies free fatty acids content present in fatty acids, which is  $1.2 \pm 0.04$  mgKOHg<sup>-1</sup> in *T. shinodae* sample. Generally, microbial lipids have higher free fatty acids that can be efficiently converted to esters using enzymatic transesterification [45].

### 4.2 Saponification value, iodine value

Combustion quality of lipids can be determined by SV and IV. SV indicates the fatty acids chain length and longer the carbon chain length, greater the combustion properties, which is measured by cetane number (CN) [46].

In the present study, *T. shinodae* lipids showed  $202 \pm 0.32$  mg/KOH (Table 5) saponification value, which signify the higher carbon chain lengths of fatty acids and ignition potential of fuel additives [39, 47]. Nouri et al. [48] reported SV of 215.3 mg/KOH from a *Sarocladium kiliense* an oleaginous fungi. On the other hand, effect of pre-treatment on substrates influences the SV. Patel et al.

[14] reported that the *Y. lipolytica* cultivated on detoxified and non-detoxified wheat straw hydrolysate showed 160.05 and 157.75 mgKOH, respectively. Similarly, supplementing glucose and xylose for cell growth and oil production (biphasic system) in *Lipomyces starkeyi* ATCC 56,304 resulted SV of 203.95 mgKOH.

The iodine value is an important parameter that determines the oxidative stability of the esters. Higher the content of unsaturated fatty acids in the oil corresponds to greater scope of oxidation and lesser oxidative stability [49]. *T. shinodae* lipids showed low iodine values  $112 \pm 0.12$  g I<sub>2</sub>/100 g (Table 5). The lower iodine value represents the higher oxidative stability of the *T. shinodae* lipids. Study conducted on IV determination using *Rhodospiridium kratochvilovae* HIMPA1 supplemented with *Cassia fistula* L. fruit pulp aqueous extract and paper industry effluent showed 16.46 mgI<sub>2</sub>/100 g and 120.017 mgI<sub>2</sub>/100 g, respectively. These studies indicate that the lipid biochemical properties predominantly depend on substrate type and pre-treatment of the lipids [50].

## 5 Conclusion

Crude glycerol (circular economy) coupled with RSM showed maximum SCO production of  $49.85 \pm 0.8\%$  with the upstream production variables of inoculum volume of 6.2 (% v/v), pH 3.6, C/N ratio of 105, 1.52 (g/L) of MgSO<sub>4</sub>, and 4.55 mM of FeSO<sub>4</sub> in 120.72 h at 30 °C. Studying the interaction effects of different production parameters on the lipid production facilitates to identify predominant variables responsible for higher lipid accumulation. The developed RSM model was exemplary with the 95.20% and 91.97% values of R<sup>2</sup> and adj. R<sup>2</sup> values, respectively. The lipid

**Table 5** *T. shinodae* chemical properties of lipids

Property	<i>T. shinodae</i>
Acid value (mg/ KOH g <sup>-1</sup> )	1.2±0.04
Iodine value (g I <sub>2</sub> /100 g)	112±0.12
Saponification value (mg/ KOH)	202±0.32

profiling of *T. shinodae* shown the presence of 61.1% saturated fatty acids and 38.9% unsaturated fatty acids. Moreover, lipid composition and biochemical properties illustrated the suitability to be used as fuel additives, surfactants and detergents due to higher chain length, ignition property, and improved oxidative stability. Therefore, bioconversion of crude glycerol for lipid synthesis using *T. shinodae* is one of the viable approaches to reduce the cost of the feedstocks.

**Acknowledgements** Authors are grateful to the Director, Indian Institute of Technology, Kharagpur for all the support rendered in the completion of the work.

**Author contributions** SPJK has conducted the experiments, analyzed the data, and drafted the paper. GVK analysed the RSM data and drafted the paper. RB conceived the research work, analysed, and edited the manuscript.

## Declarations

**Conflict of interest** The authors declare no competing interests.

## References

- Banerjee R, Kumar SPJ, Mehendale N, Sevda S, Garlapati VK (2019) Intervention of microfluidics in biofuel and bioenergy sectors: technological considerations and future prospects. *Renew Sustain Energy Rev* 101:548–558. <https://doi.org/10.1016/j.rser.2018.11.040>
- Gujjala LKS, Kumar SPJ, Talukdar B, Dash A, Kumar S, Sherpa KCH, Banerjee R (2017) Biodiesel from oleaginous microbes: opportunities and challenges. *Biofuels* 1: 1–15. <https://www.tandfonline.com/doi/abs/https://doi.org/10.1080/17597269.2017.1402587>
- Cho HU, Park JM (2018) Biodiesel production by various oleaginous microorganisms from organic wastes. *Bioresour Technol* 256:502–508. <https://doi.org/10.1016/j.biortech.2018.02.010>
- Kumar SPJ, Banerjee R (2019) Enhanced lipid extraction from oleaginous yeast biomass using ultrasound assisted extraction: a greener and scalable process. *Ultrason Sonochem* 52:25–32. <https://doi.org/10.1016/j.ultsonch.2018.08.003>
- Kumar SPJ, Kumar NS, Chintagunta AD (2020) Bioethanol production from cereal crops and lignocelluloses rich agro-residues: prospects and challenges. *SN Appl Sci* 10:1–1. <https://doi.org/10.1007/s42452-020-03471-x>
- Vlysidis A, Binns M, Webb C, Theodoropoulos C (2011) A techno-economic analysis of biodiesel biorefineries: assessment of integrated designs for the co-production of fuels and chemicals. *Energy* 36:4671–4683. <https://doi.org/10.1016/j.energy.2011.04.046>
- Varrone C, Liberatore R, Crescenzi T, Izzo G, Wang A (2013) The valorization of glycerol: economic assessment of an innovative process for the bioconversion of crude glycerol into ethanol and hydrogen. *Appl Energy* 105:349–357. <https://doi.org/10.1016/j.apenergy.2013.01.015>
- Kumari A, Mahapatra P, Garlapati VK, Banerjee R (2009) Enzymatic transesterification of Jatropha oil. *Biotechnol Biofuels* 2:1. <https://doi.org/10.1186/1754-6834-2-1>
- Garlapati VK, Kant R, Kumari A, Mahapatra P, Das P, Banerjee R (2013) Lipase mediated transesterification of *Simarouba glauca* oil: a new feedstock for biodiesel production. *Sustain Chem Process* 1:11. <https://doi.org/10.1186/2043-7129-1-11>
- Garlapati VK, Mahapatra SB, Mohanty RC, Das P (2021) Transesterified *Olaix scandens* oil as a bio-additive: production and diesel engine performance studies. *Tribol Int* 153:106653. <https://doi.org/10.1016/j.triboint.2020.106653>
- Banerjee R, Chintagunta A, Ray S (2017) A cleaner and eco-friendly bioprocess for enhancing reducing sugar production from pineapple leaf waste. *J Clean Prod* 149:387–395. <https://doi.org/10.1016/j.jclepro.2017.02.088>
- Talebian-Kiakalaieh A, Amin NAS, Mazaheri H (2013) A review on novel processes of biodiesel production from waste cooking oil. *Appl Energy* 104:683–710. <https://doi.org/10.1016/j.apenergy.2012.11.061>
- Souza KST, Ramos CL, Schwan RF, Dias DR (2016) Lipid production by yeasts grown on crude glycerol from biodiesel industry. *Prep Biochem Biotechnol* 1–7. <https://doi.org/10.1080/10826068.2016.1244689>
- Patel A, Arora N, Mehtani J, Pruthi V, Pruthi PA (2017) Assessment of fuel properties on the basis of fatty acid profiles of oleaginous yeast for potential biodiesel production. *Renew Sustain Energy Rev* 77:604–616. <https://doi.org/10.1016/j.rser.2017.04.016>
- Wu H, Li Y, Chen L, Zong M (2011) Production of microbial oil with high oleic acid content by *Trichosporon capitatum*. *Appl Energy* 88:138–142. <https://doi.org/10.1016/j.apenergy.2010.07.028>
- Sharma D, Garlapati VK, Goel G (2016) Bioprocessing of wheat bran for the production of lignocellulolytic enzyme cocktail by *Corylidia pannosa* under submerged conditions. *Bioengineered* 7(2):88–97. <https://doi.org/10.1080/21655979.2016.1160190>
- Bezerra MA, Santelli RE, Oliveiraa EP, Villar LS, Escalera LA (2008) Response surface methodology (RSM) as a tool for optimization in analytical chemistry. *Talanta* 76:965–977. <https://doi.org/10.1016/j.talanta.2008.05.019>
- Chauhan M, Chauhan RS, Garlapati VK (2013) Modelling and optimization studies on a novel lipase production by *Staphylococcus arlettae* through submerged fermentation. *Enzyme Res* 2013: Article ID 353954, 1–8. <https://doi.org/10.1155/2013/353954>
- Kumar SPJ, Banerjee R (2013) Optimization of lipid enriched biomass production from oleaginous fungus using response surface methodology. *Indian J Exp Biol* 51: 979–983. <http://nopr.niscair.res.in/handle/123456789/23466>
- Gorte O, Kugel M, Ochsenreither K (2020) Optimization of carbon source efficiency for lipid production with the oleaginous yeast *Saitozyma podzolica* DSM 27192 applying automated continuous feeding. *Biotechnol Biofuels* 13:181. <https://doi.org/10.1186/s13068-020-01824-7>
- Awad D, Bohnen F, Mehlmner N, Brueck T (2019) Multi-factorial-guided media optimization for enhanced biomass and lipid formation by the oleaginous yeast *Cutaneotrichosporon oleaginosus*. *Front Bioeng Biotechnol* 26(7):54. <https://doi.org/10.3389/fbioe.2019.0005426>
- Jacquet N, Haubruge E, Richel A (2015) Production of biofuels and biomolecules in the framework of circular economy: a regional case study. *Waste Manage Res* 33:1121–1126. <https://doi.org/10.1177/0734242X15613154>
- Kumar SPJ, Gujjala LKS, Dash A, Talukdar B, Banerjee R (2017) Biodiesel production from lignocellulosic biomass using oleaginous microbes. In: Kuila A, Sharma V (eds) *Lignocellulosic biomass production and industrial applications*. Wiley, New York, pp 65–92
- Salakkam A, Webb C (2015) The inhibition effect of methanol as a component of crude glycerol on the growth rate of *Cupriavidus*

- necator* and other microorganisms. *Biochem Eng J* 98:84–90. <https://doi.org/10.1016/j.bej.2015.02.024>
25. Uprety BK, Dalli SS, Rakshit SK (2017) Bioconversion of crude glycerol to microbial lipid using a robust oleaginous yeast *Rhodospiridium toruloides* ATCC 10788 capable of growing in the presence of impurities. *Energy Convers Manage* 135:117–128. <https://doi.org/10.1016/j.enconman.2016.12.071>
  26. Folch J, Lees M, Stanley GHS (1957) A simple method for the isolation and purification of total lipids from animal tissues. *J Biol Chem* 226:497–509
  27. Garlapati VK, Banerjee R (2010) Optimization of lipase production using differential evolution. *Biotechnol Bioproc E* 15:254–260. <https://doi.org/10.1007/s12257-009-0163-3>
  28. Garlapati VK, Kumari A, Mahapatra P, Banerjee R (2013) Modeling, simulation and kinetic studies of solvent-free biosynthesis of benzyl acetate. *J Chem* 2013: Article ID 451652, 1–9, doi: <https://doi.org/10.1155/2013/451652>.
  29. Forfang K, Zimmermann B, Kosa G, Kohler A, Shapaval V (2017) FTIR spectroscopy for evaluation and monitoring of lipid extraction efficiency for oleaginous fungi. *PLoS ONE* 12:e0170611. <https://doi.org/10.1371/journal.pone.0170611>
  30. Sorate KA, Bhale PV (2015) Biodiesel properties and automotive system compatibility issues. *Renew Sustain Energy Rev* 41:777–798. <https://doi.org/10.1016/j.rser.2014.08.079>
  31. Polburee P, Yongmanitchai W, Honda K, Ohashi T, Yoshida T, Fujiyama K, Limtong S (2016) Lipid production from biodiesel-derived crude glycerol by *Rhodospiridium fluviale* DMKU-RK253 using temperature shift with high cell density. *Biochem Eng J* 112:208–218. <https://doi.org/10.1016/j.bej.2016.04.024>
  32. Jernejc K, Legisa M (2002) The influence of metal ions on malic enzyme activity and lipid synthesis in *Aspergillus niger*. *FEMS Microbiol Lett* 217:185–190. <https://doi.org/10.1111/j.1574-6968.2002.tb11473.x>
  33. Saenge C, Cherisilp B, Suksarogee TT, Bourtoom T (2011) Efficient concomitant production of lipids and carotenoids by oleaginous red yeast *Rhodotorula glutinis* cultured in palm oil mill effluent and application of lipids for biodiesel production. *Biotechnol Bioprocess Eng* 16:23–33. <https://doi.org/10.1007/s12257-010-0083-2>
  34. Immelman M, Du Preez JC, Kilian SG (1997) Effect of C: N ratio on gamma-linolenic acid production by *Mucor circinelloides* grown on acetic acid. *Syst Appl Microbiol* 20:158–164. [https://doi.org/10.1016/S0723-2020\(97\)80061-6](https://doi.org/10.1016/S0723-2020(97)80061-6)
  35. Man L, Behera SK, Park HS (2010) Optimization of operational parameters for ethanol production from Korean food waste leachate. *Int J Environ Sci Tech* 7:157–164. <https://doi.org/10.1007/BF03326127>
  36. Xu J, Zhao X, Wang W, Du W, Liu D (2012) Microbial conversion of biodiesel byproduct glycerol to triacylglycerols by oleaginous yeast *Rhodospiridium toruloides* and the individual effect of some impurities on lipid production. *Biochem Eng J* 65:30–36. <https://doi.org/10.1016/j.bej.2012.04.003>
  37. Saenge C, Cherisilp B, Suksarogee TT, Bourtoom T (2011) Potential use of oleaginous red yeast *Rhodotorula glutinis* for the bioconversion of crude glycerol from biodiesel plant to lipids and carotenoids. *Process Biochem* 46:210–218. <https://doi.org/10.1016/j.procbio.2010.08.009>
  38. Zhang J, Bilal M, Liu S, Zhang J, Lu H, Luo H, Luo C, Shi H, Hafiz M, Iqbal N, Zhao Y (2019) Sustainable biotransformation of oleic acid to 10-hydroxystearic acid by a recombinant oleate hydratase from *Lactococcus garvieae*. *Process* 7:326. <https://doi.org/10.3390/pr7060326>
  39. Knothe G, Bagby MO, Ryan TW (1998) Precombustion of fatty acids and esters of biodiesel. A possible explanation for differing cetane numbers. *J Amer Oil Chem Soc* 75:1007–1013. <https://doi.org/10.1007/s11746-998-0279-1>
  40. Dunn RO, Knothe GH (2003) Oxidative stability of biodiesel/jet fuel blends by oil stability index (osi) analysis. *J Am Oil Chem Soc* 80:1047–1048. <https://doi.org/10.1007/s11746-003-0818-6>
  41. Rabelo SN, Ferraz VP, Oliveira LS, Franca AS (2015) FTIR analysis for quantification of fatty acid methyl esters in biodiesel produced by microwave-assisted transesterification. *Int J Environ Sci Dev* 6:964. <https://doi.org/10.7763/IJESD.2015.V6.730>
  42. Soares IP, Rezende TF, Silva RC, Castro EV, Fortes IC (2008) Multivariate calibration by variable selection for blends of raw soybean oil/biodiesel from different sources using Fourier transform infrared spectroscopy (FTIR) spectra data. *Energy Fuels* 22:2079–2083. <https://doi.org/10.1021/ef700531n>
  43. Dubé MA, Zheng S, McLean DD, Kates M (2004) A comparison of attenuated total reflectance-FTIR spectroscopy and GPC for monitoring biodiesel production. *J Am Oil Chem Soc* 81:599–603. <https://doi.org/10.1007/s11746-006-0948-x>
  44. Dean AP, Sigee DC, Estrada B, Pittman JK (2010) Using FTIR spectroscopy for rapid determination of lipid accumulation in response to nitrogen limitation in freshwater microalgae. *Bioresource Technol* 101:4499–4507. <https://doi.org/10.1016/j.biortech.2010.01.065>
  45. Ramírez-Verduzco LF, Rodríguez-Rodríguez JE, Jaramillo-Jacob ADR (2012) Predicting cetane number, kinematic viscosity, density and higher heating value of biodiesel from its fatty acid methyl ester composition. *Fuel* 91:102–111. <https://doi.org/10.1016/j.fuel.2011.06.070>
  46. Datta A, Mandal BK (2016) A comprehensive review of biodiesel as an alternative fuel for compression ignition engine. *Renew Sustain Energy Rev* 57:799–821. <https://doi.org/10.1016/j.rser.2015.12.170>
  47. Gopinath A, Puhan S, Nagarajan G (2009) Theoretical modeling of iodine value and saponification value of biodiesel fuels from their fatty acid composition. *Renew Energy* 34:1806–1811. <https://doi.org/10.1016/j.renene.2008.11.023>
  48. Nouri H, Moghimi H, Rad MN, Ostovar M, Mehr SS, Ghanaatian F, Talebi AF (2019) Enhanced growth and lipid production in oleaginous fungus, *Sarocladium kiliense* ADH17: study on fatty acid profiling and prediction of biodiesel properties. *Renew Energy* 135:10–20. <https://doi.org/10.1016/j.renene.2018.11.104>
  49. Vicente G, Martinez M, Aracil J (2004) Integrated biodiesel production: a comparison of different homogeneous catalysts systems. *Bioresource Technol* 92:297–305. <https://doi.org/10.1016/j.biortech.2003.08.014>
  50. Toscano G, Riva G, Foppa Pedretti E, Duca D (2012) Vegetable oil and fat viscosity forecast models based on iodine number and saponification number. *Biomass Bioenergy* 46:511–516. <https://doi.org/10.1016/j.biombioe.2012.07.009>
  51. Tao BY (2007) Industrial applications for plant oils and lipids. In: Shang-Tian Y (ed) *Bioprocessing for value-added products from renewable resources*. Elsevier Science, USA, pp 611–627

**Publisher's note** Springer Nature remains neutral with regard to jurisdictional claims in published maps and institutional affiliations.